Evaluation of the AZ31 cyclic elastic-plastic behaviour under multiaxial loading conditions

V. Anes

Instituto Superior Técnico, University of Lisbon
4140.fatigue@gmail.com

L. Reis, M. Freitas

IDMEC & ICEMS, Instituto Superior Técnico, University of Lisbon,
luis.g.reis@ist.utl.pt, mfreitas@dem.ist.utl.pt

ABSTRACT. Components and structures are designed based in their material's mechanical properties such as Young's modulus or yield stress among others. Often those properties are obtained under monotonic mechanical tests but rarely under cyclic ones. It is assumed that those properties are maintained during the material fatigue life. However, under cyclic loadings, materials tend to change their mechanical properties, which can improve their strength (material hardening) or degrade their mechanical capabilities (material softening) or even a mix of both. This type of material behaviour is the so-called cyclic plasticity that is dependent of several factors such as the load type, load level, and microstructure.

This subject is of most importance in design of structures and components against fatigue failures in particular in the case of magnesium alloys. Magnesium alloys due to their hexagonal compact microstructure have only 3 slip planes plus 1 twining plane which results in a peculiar mechanical behaviour under cyclic loading conditions especially under multiaxial loadings. Therefore, it is necessary to have a cyclic elastic-plastic model that allows estimating the material mechanical properties for a certain stress level and loading type.

In this paper it is discussed several aspects of the magnesium alloys cyclic properties under uniaxial and multiaxial loading conditions at several stress levels taking into account experimental data.

A series of fatigue tests under strain control were performed in hour glass specimens test made of a magnesium alloy, AZ31BF. The strain/stress relation for uniaxial loadings, axial and shear was experimentally obtained and compared with the estimations obtained from the theoretical elastic-plastic models found in the state-of-the-art. Results show that the AZ31BF magnesium alloy has a peculiar mechanical behaviour, which is quite different from the steel one. Moreover, the state of the art cyclic models do not capture in full this peculiar behaviour, especially the cyclic magnesium alloys anisotropy. Further, an analysis is performed to identify the shortcomings inherent to the actual cyclic models in the capture of the magnesium alloys cyclic behaviour. Several conclusions are drawn.

KEYWORDS. Magnesium alloys; AZ31B-F; Cyclic elastic-plastic model; Multiaxial loadings; Experimental tests.

INTRODUCTION

Knowing the material stress state under any kind of loadings is of utmost importance since the interpretation of the mechanical behaviour is based in that stress state[1, 2]. In the design of mechanical components it is used the Hooke's law that relates linearly the stress and deformation. This law is only valid in elastic regimes and assumes that the relation between stress and deformation is always constant. However, even in elastic regimes, the material mechanical properties may change. This variation is related with the materials cyclic plasticity where the strength of the materials changes with the loading type and with the load level [2, 3]. Also the material type has huge influence in the response to the load type. It was observed that the number of slip plans have an huge influence on the cyclic behaviour, for example, magnesium alloys have only 3 slip plans (or slip directions) against 12 found in steel alloys [4]. This is why these two types of materials have a cyclic mechanical behaviour so different. One way to interpret the variation of the cyclic mechanical properties is to analyse the hysteresis loop resulting from several loading paths at several stress levels. From these hysteresis loops can be inspected the yield stresses in tension and compression; in steels the yield stresses in tension and compression are the same or similar, but for other types of materials those stresses it may be quite different, which is the case of magnesium alloys. Other important parameter that can be obtained from a hysteresis loop is the total strain for a certain stress level. As seen, in the aforementioned cyclic yield stress cases, also the total strain in tension and in compression may be different for the same stress level in tension and compression. This result indicates that the plastic strain in tension and compression are different as well as the elastic ones. The cyclic yield stresses are usually below the static ones, thus the aforementioned cyclic behaviours can occur with stresses below the static yield stress. Thus a key question may be raised: What is the real stress state of the material under cyclic loading conditions? There is some way to know those stress states?

The answer to these questions is of utmost importance because it is only possible to reach reliable conclusions about the material mechanical behaviour knowing the real relation between stress and strain in any loading condition. This relation depends on the stress level and of the load type. There are plenty of plasticity models in literature but the phenomenological ones covering the elastic-plastic behaviour under cyclic conditions are very few especially the ones that capture cyclic plasticity under multiaxial loading conditions. Therefore, cyclic hardening/softening and cyclic creep under multiaxial loading conditions remains a subject that needs further research. This is so because elastic-plastic models must be made based in experimental tests. It is only possible know the material cyclic behaviour by testing them. It is required to perform a kind of mapping of the material cyclic behaviour under cyclic loadings, especially under multiaxial loading conditions. Plasticity models usually have a yield function, a back stress function, and a kinematic function. These functions aim to capture the permanent deformation and change on the mechanical properties of the material.

Most of those plasticity models are strictly based in the static yield stress and assumes that the yield stress in tension and compression are equal. In other words, they assume that the difference between yield stresses in tension and compression is always maintained equal, trying to cover in that way the Bauschinger effect. Moreover, their yield stress is based in the von Mises equivalent stress, which assumes that the relation between the deformation in axial and shear is given by $\sqrt{3}$, which is not true for certain materials under cyclic loading conditions[3, 5, 6].

Therefore, that kind of plasticity models are not suitable to be used in cyclic analysis for materials with different yield stresses in tension and compression. In fact, commercial finite element packages do not have intrinsic cyclic plasticity models to modulate such type of materials. The only way to account the special cyclic behaviour, using commercial FEA packages, is to implement an external routine that can update the material cyclic response. Generally, the cyclic plasticity models are constitutive models that are modelled by numerical tools. They can be divided in six major groups, four groups based in yield surface [7-10], one based in overlapping models [11] and other one based in endochroic models[12]. Models with one yield surface tend to be more robust than others that have two or more yield surfaces. One important issue in this subject is that all constitutive elastic-plastic models do not capture the materials anisotropy; they purely ignore this important material behaviour[4]. Therefore, materials that have a cyclic anisotropic behaviour such as magnesium alloys will not be well modelled using these models. Also, they do not capture the influence of the strain rate nor the temperature effect in the cyclic behaviour of the materials. Moreover, the cyclic models available in literature do not cover an important aspect of mechanical components, which is the anisotropy from the manufacturing process. The anisotropy in the materials may result from several reasons; for instance, it is well known the directional dependence of the mechanical properties in a sheet of metal. That anisotropy is the result from the lamination process, also in an extruded rod, the longitudinal properties will be different from the transversal ones, and this difference is the result of the material alignment in the extrusion process. In this sense, it is quite difficult to find in the field, manufactured materials that have isotropic properties especially at surface. However, it is at surface where usually the fatigue phenomenon occurs; therefore

it is of utmost importance to know the local cyclic stress states of the material[16]. The isotropic hypothesis considered in the state of the art of the elastic-plastic models in reality is an approximation to the material stress state

Another type of anisotropy found in the materials is the one that results from the material response to the loading type. The rearrangements of the material microstructure have some preferable directions that are related with the loading type and the microstructure slip system. One example is the non-proportional hardening, which is the result of non-proportional loadings. In this type of loading all slip plans are activated however, the hardening effect it may be not equal in all directions [10, 13]. Also within the non-proportional loadings there exist several non-proportionality levels, which also contribute to different anisotropy types. The research problem is that besides the actual cyclic elastic-plastic models do not cover the anisotropy that resulted from the manufacturing process also does not cover the anisotropy that results from the loading type. This is a huge shortcoming in these elastic-plastic models found in literature being not advisable their use in fatigue life assessment especially under multiaxial loading conditions. The objective of this work is to implement an elastic-plastic numerical model in order to modelling the materials cyclic elastoplasticity under complex multiaxial loadings. In order to do that, was selected the AZ31 magnesium alloy due to their peculiar mechanical behaviour and because it is a magnesium alloy used in the industry. Also in this study it is presented methodologies to deal with this kind of materials i.e. hexagonal closed packed. The ultimate goal is to reach a numeric tool that can be used in generic HCP materials and used in synergy with a commercial finite element packages (external routine). Results show that the numerical methodologies implemented allows modulating the AZ31 magnesium alloy mechanical behaviour under uniaxial loading conditions with acceptable accuracy; moreover under multiaxial conditions the achieved results are quite similar to the ones obtained with the Jiang & Sehitoglu plasticity model. However, additional multiaxial stress-strain experiments are needed to adjust and validate the considered multiaxial hypothesis.

THEORETICAL DEVELOPMENT

The Jiang & Sehitoglu plasticity model is a non-linear kinematic hardening model that incorporates an Armstrong-Frederick type hardening rule, in order to capture the Bauschinger effect on the cyclic plastic deformation. This model was implemented with the purpose of modulating the cyclic ratcheting phenomena that is a progressive and directional plastic deformation when a material is subjected to asymmetric loadings under stress-controlled regimens, which makes this model a good candidate to model the magnesium alloy elastic-plastic behaviour. One peculiarity associated with this model is related to the inclusion of a non-proportional hardening parameter, where the non-proportional hardening results in an additional resistance of the material to plastic deformation under non-proportional loading. Also, it is introduced the memory concept on the material behaviour simulation in order to describe the strain range dependency in the cyclic hardening. The Jiang & Sehitoglu plasticity model also considers several others physical mechanisms, such as: Yield function, which considers a combinations of stresses that will lead to plastic deformations; Flow rule, creates a relationship between the stresses and plastic strains during plastic deformation; hardening rule, defines the yield criterion changes under plastic straining; stress relaxation and load redistribution in the stressed volume.

The Jiang & Sehitoglu plasticity model routine used in this study has as input the strain loading paths and the AZ31B-F magnesium alloy mechanical properties; the analysis was performed under strain control conditions. This routine was implemented by considering the stress/strain tensor on an elemental cube, therefore it is not applied to a specimen test modelled in finite element. The mechanical properties considered as input in this program are: Young's modulus, cyclic Strength coefficient, proportional cyclic strain hardening exponent, cyclic strength coefficient at 90 degrees, non-proportional cyclic strain hardening exponent at 90 degrees, poison coefficient and shear modulus. It is assumed that the cyclic hardening exponent is constant for proportional and non-proportional loads. The non-proportional cyclic strength at 90° is calculated considering the Kanazawa non-proportional constant, with a value $\alpha = 0.1$.

In order to cover all the phenomena discussed in previous sections, it is used the experimental hysteresis loop data performed under cyclic strain control in pure axial loading and pure shear loading conditions. The objective is to achieve a numeric model capable to estimate the relation between stress-strain in uniaxial and biaxial loading conditions under a realistic strain range. The constraints aforementioned means that the numeric model only will modulate the applied strain if it belongs to the strain ranges established in the experimental tests. However, in this study the experimental tests were performed from elastic strains until reach total strains with high plasticity resulting in the specimen collapse at very few load cycles. Thus, here a realistic stress-strain relation is covered. This does not mean that were made experimental tests for all total strain levels, instead were selected several total-strains that will allow to perform valid numeric regressions. These values were carefully selected and used in the experimental cyclic tests. From experiments, was found that the AZ31 magnesium alloy hysteresis loops can be approximated with very acceptable results using a third degree polynomial

interpolation for any value of total-strain. In order to perform those interpolations it is considered several specific points on the hysteresis loop, thus for the compression polynomial branch, the points 1,2,3 and 4 shown on Fig. 1 are used; for the tension polynomial branch, are used the points 4,5,6 and 1. These polynomials capture the twinning, de-twinning and slip effect at each total strain level. Thus the hysteresis loop at specific total strain is given by the following equations for compression (Eq. (1)) and tension (Eq. (2)) respectively.

$$a\left(\varepsilon_{total}\right)\cdot\varepsilon_{total}^{3} + b\left(\varepsilon_{total}\right)\cdot\varepsilon_{total}^{2} + c\left(\varepsilon_{total}\right)\cdot\varepsilon_{total}^{1} + d\left(\varepsilon_{total}\right) \tag{1}$$

$$e\left(\varepsilon_{total}\right)\cdot\varepsilon_{total}^{3} + f\left(\varepsilon_{total}\right)\cdot\varepsilon_{total}^{2} + g\left(\varepsilon_{total}\right)\cdot\varepsilon_{total}^{1} + h\left(\varepsilon_{total}\right) \tag{2}$$

From here, the problem is reduced to find the polynomial parameter values in compression and tension for any total strains within the experimental range. In order to do that, was considered the polyfit Matlab routine to obtain these values; this routine has as arguments the stress-strain values inherent to the points 1,2,3 and 4 for compression and 4,5,6 and 1 for tension. From here the problem is reduced to find the function, which relates the arguments of the polyfit routine with the applied load i.e. the applied total strain. The referred points are related to the specific mechanical behaviour found under elastic-plastic regimes. The points 1 and 4 can be considered as values from an experimental yield function, where point 1 come from the tension /compression load direction and point 4 come from the compression/tension. Moreover, the points 2 and 5 are the plastic strains, which can be related to the typical isotropic/kinematic hardening models found on constitutive plastic models. The points 3 and 6 can be related to the back-stress concept which is the stress needed to reduce plastic strains to zero. Eq.(s) 3 and 4 presents de polyfit Matlab function for the compression and tension loading branches, respectively.

$$\left[a\left(\varepsilon_{total}\right),b\left(\varepsilon_{total}\right),c\left(\varepsilon_{total}\right),d\left(\varepsilon_{total}\right)\right] = polyfit\left(\left(\sigma,\varepsilon_{total}\right)_{1},\left(0,\varepsilon_{plastic}\right)_{2},\left(\sigma,0\right)_{3},\left(\sigma,-\varepsilon_{total}\right)_{4}\right) \tag{3}$$

$$\left[e\left(\varepsilon_{total}\right),f\left(\varepsilon_{total}\right),g\left(\varepsilon_{total}\right),h\left(\varepsilon_{total}\right)\right] = polyfit\left(\left(\sigma,-\varepsilon_{total}\right)_{4},\left(0,\varepsilon_{plastic}\right)_{5},\left(\sigma,0\right)_{6},\left(\sigma,\varepsilon_{total}\right)_{1}\right) \tag{4}$$
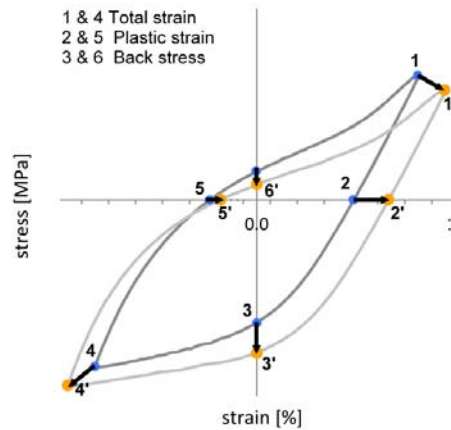

Figure 1: Third degree polynomial interpolation reference points, in tension and compression loading directions for two consecutive hysteresis loops.

The core concept of the numeric model presented here is based on obtaining the functions relating the variation of the polynomial interpolation points with the total-strain variation. In this work, those values were determined by considering a third degree polynomial fitting equation for the branches in tension and compression, obtained from the experimental data hysteresis loop. With these experimental data, it was achieved the aforementioned functions by interpolation to estimate the variation of the polynomial regression arguments with the total strain variation. At the current state of the model, the biaxial elastic-plastic behaviour is estimated by considering separately the biaxial loading strains (axial and shear), which is a simplification. With this simplification, it is assumed that the axial stress and the shear stress do not contribute to each other in terms of cyclic plasticity. However, biaxial elastic-plastic experiments are in progress to be used in the upgrade of the current model. Similarly to the Jiang & Sehitoglu plasticity model routine, the proposed approach also is related to an elemental cube; therefore, all conclusions made here are related to an infinitesimal material point.

MATERIALS AND METHODS

The material used in this study was the magnesium alloy AZ31-B. This alloy was acquired in the form of rods with 26 mm of diameter and 1000 mm in length. The rods were extruded in a temperature range of 360 to 382 °C with an extrusion speed of 50.8 mm/s. The applied extrusion ratio was about six, and after extrusion the alloy was air quenched. The tested specimens were machined in the extrusion/longitudinal direction and polished with decrease levels of sandpaper.

An Instron servo-hydraulic testing machine was used to perform the cyclic tests at strain control regime with R=-1 with a sinusoidal waveform. Several total strain amplitudes were considered and obtained at the same strain rate. The strain rate considered in this study was about 0,003 [1/s], which is a value lower than the limit, from which the strain rate affects the cyclic strain behaviour of the magnesium alloys. The strain results were measured with a biaxial extensometer with a gauge length equal to 12.5 mm. The strain controlled tests were made considering the following total strains: 0.3%, 0.5%, 0.7%, 0.9%, 1.2% and 1,4%. Each cyclic test was considered concluded at the occurrence of the specimen total separation. To evaluate the influence of the microstructure in the mechanical behaviour four biaxial loading paths were considered, please see Fig. 2. The first loading case is a pure uniaxial tensile test, case PT; the second one is a pure shear loading, case PS. These loading paths were implemented in experiments and in the numerical analysis. The PP is a 45° proportional biaxial loading and the OP case is a 90° out-of-phase loading path. These biaxial loading paths were implemented only in the numerical analysis. The experimental tests were performed at room temperature and ended when the specimens were totally separated.
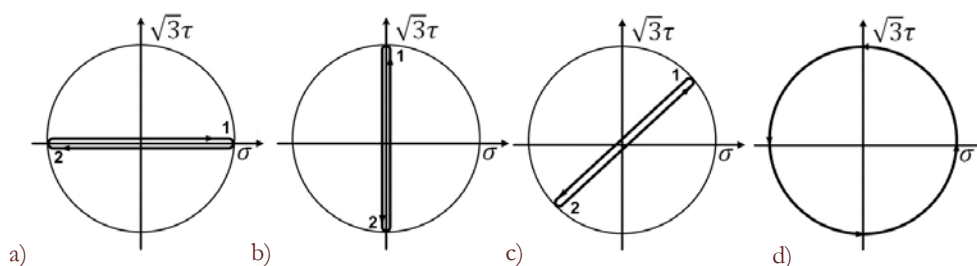

Figure 2: Loading paths: a) case PT, b) case PS, c) case PP and d) case OP.

RESULTS AND DISCUSSION

Fig. 3 shows the variation of several variables inherent to the magnesium elastic-plastic mechanical behaviour in function of total strain values under cyclic loading conditions obtained from experimental tests. Fig. 3a) and 3b) show the results for the axial loading case, can be seen that the compression and tension have a similar behaviour for total strains lower than 0.4% where the values of the back-stress are negligible. At total strains, with values between 0.4% and 0.6 %, the curves in tensile and compression have a cyclic hardening behaviour but with different hardening rates. This observation corroborates the results shown on Fig. 3b) where the plastic strain increase is followed by an axial stress increase. Moreover, from tensile stress curve and from the tensile plastic strain can be concluded that the plastic strain is increasing with a tensile stress decrease which indicates that the material softened for this total strain range i.e. between 0.6% and 1.4 %. In addition, it can be concluded that under compression, the material is always under a hardening regime. From here, can be concluded that the magnesium alloys harden, softens and have a mixed behaviour in axial loading regimes. From the axial results, Fig. 3a), also can be concluded that the back-stress in compression is greater than the one found in tension for a total strain greater than 0.6%.For total-strains with values lower than 0.6%, the back-stress in tension is greater than the one verified at compression. From here can be concluded that the back stresses in axial loading conditions operates differently in tension and compression. Therefore, the plastic behaviour is dependent on the total strain amplitude. Also the plastic strain in tension is always greater than the compressive one (see Fig. 3).The pure shear results shown in Fig. 3c) and 3d) indicate quasi-overlapping curves in the case of total-strains versus shear stresses. These results show that the shear-strain hysteresis loops are quasi symmetrical in any total shear strain. However, from the back-stress curves in shear, can be seen that the back stress has a different total shear stress evolution, indicating that the shear direction of the first cycle loading influences these results. This feature also can be observed in Fig. 3c) where the total shear strain versus plastic strain curves are not overlapped as expected. Despite the shear hysteresis loop be symmetrical the plastic strains are greater in one direction than in another. However, the curves have a similar shape, also

leading to conclude that the first loading cycle has influence on the hysteresis inherent plasticity. This issue is related to the sequential effect on the elastic-plastic behaviour. This experimental evidence indicates one more variable to take into account in the numeric model only identified by experimental tests. However, this sequential effect identified for one shear direction it can be extrapolated for the other one, considering the same experimental data.
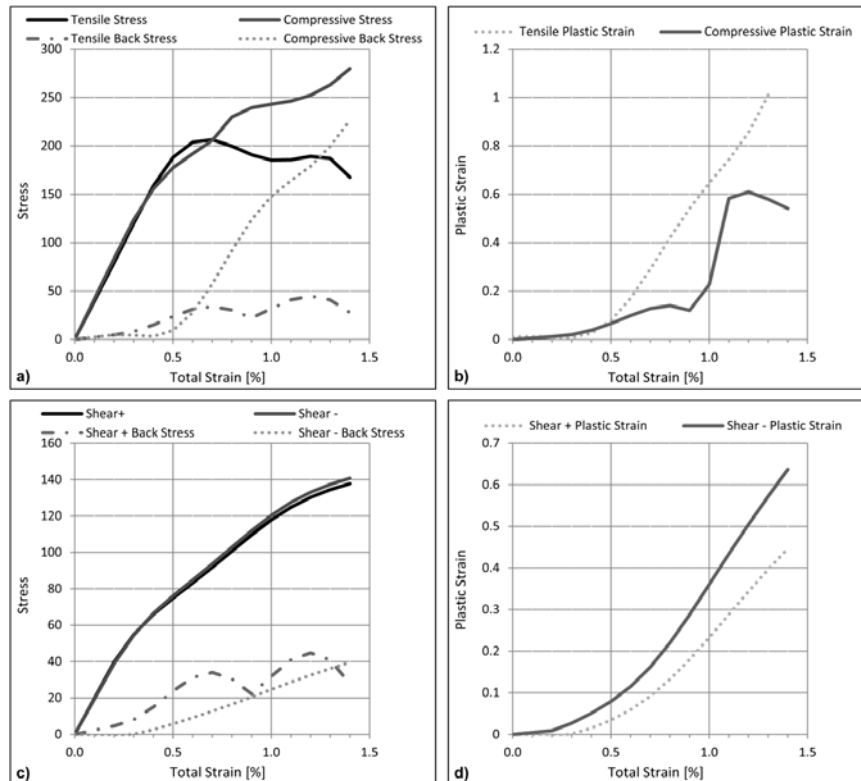

Figure 3: Plastic strains and back stresses vs total strains under uniaxial loading conditions a) and b) axial loading case and c) and d) shear loading case.

Fig. 4 shows the experimental and numerical hysteresis loops for the uniaxial loading cases. Fig. 4a) and 4b) show the experimental and numerical results of the pure axial loading path under several total strains. The pure shear results are shown in Fig. 4c) and 4d). The total strain values selected to perform the numerical analyses were the same used in the experimental tests in order to analyse the accuracy of the numeric hysteresis loop estimation.

Since the numeric model here presented is based on the uniaxial experimental tests it is expected that the results be quite similar, if the assumptions made on the numeric model definition are true. Nevertheless, the estimations are quite acceptable for the uniaxial loading cases, confirming that the hysteresis loops in pure axial and pure shear loading conditions can be approximated by a third degree polynomial function. In order to avoid confusion in the graphs interpretation was not considered here the representation of the hysteresis loops with total strains different of the experimental ones. However, the numerical model can estimate any hysteresis loop within the [0% to 1.4%] total strain range under uniaxial loading conditions. From the axial hysteresis loops can be identified the asymmetry inherent to the different mechanical behaviours found in tension and compression. Moreover, the shear hysteresis loops are quasi-symmetric. Fig. 5a) and 5b) shows the numeric results for 0.4% of total axial strain and 0.23 % of total shear strain. Fig. 5a) shows a comparison between the numerical model and the Jiang plasticity model for the case of pure axial loading. From that comparison can be concluded that the Jiang hysteresis loop is more open than the experimental one, indicating the existence of plastic strain and back stresses that in reality are not there. Moreover, the stresses estimated by the Jiang model at the maximum total strain in uniaxial axial loading, please see Fig. 5b), are inferior to the ones obtained from the numerical model. Considering the pure shear analysis, present in Fig. 5b) the Jiang model continues to estimate inferior stresses at the maximum total shear strains. The biaxial loading cases are shown in Fig. 5c) and 5d). At the present work state, is not possible to compare the numerical estimates with the experimental results, however the numerical model implemented can be compared with the Jiang plasticity model. For the PP loading case, can be concluded that the slope of the hysteresis loops and inherent orientations are different in both numeric models. The difference observed in the slope

can result from the considered scale factor between axial and shear strains used in the Jiang model. Usually, the von Mises stress scale factor is used but the Jiang model uses 0.5 as stress scale factor against the 0.577 found in the von Mises yield criterion. The numerical model presented here, considers the axial and shear total strain separately in order to estimate the mechanical behaviour as if they had been applied at the same time. The physical meaning of this simplification considers that the stress needed in shear and axial directions to make the same plastic strain is the same, which is not true for most metallic materials. This relation can only be found by performing biaxial stress-strain tests under an elastic-plastic regimen. Fig. 5d) shows the results for the fully out-of-phase loading case; in this case, the estimations of both numerical models are quite similar. The Jiang's model estimations are within of the numerical model results due to the fact that the Jiang model calculates lower stresses, for the same total strain. However, in the stress space, both estimations for the loading path have a similar shape for the same total strain level presented in Fig. 5d).
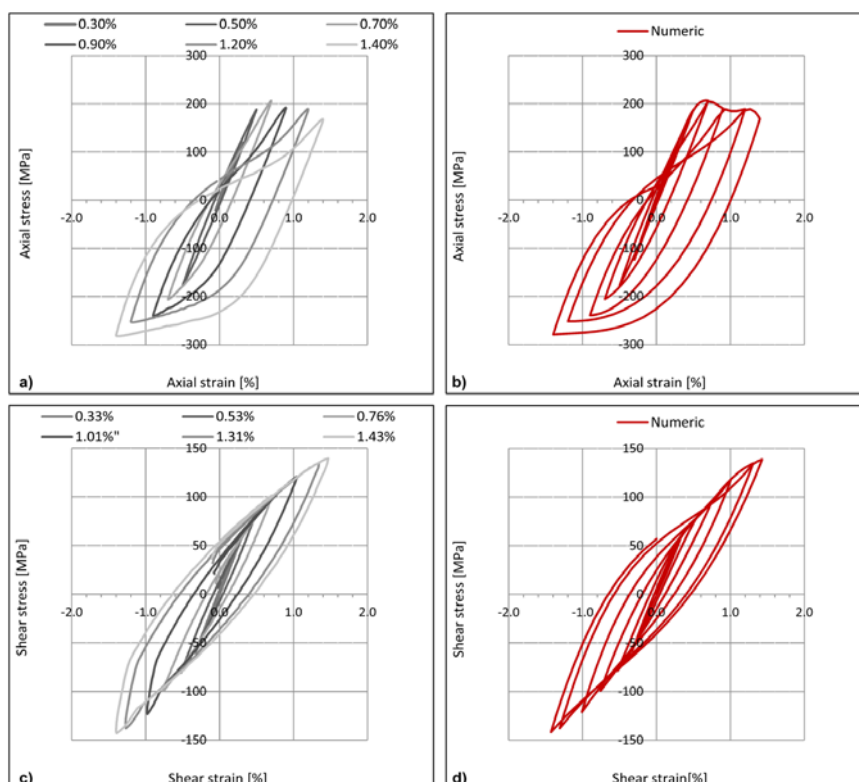

Figure 4: AZ31 experimental and numeric cyclic behavior a) Axial experimental stress/strain evolution b) Numeric results for axial stress/strain hysteresis loops c) Shear experimental stress/strain evolution d) Numeric estimation for shear stress/strain hysteresis loops.

Fig. 6 shows the numeric results for 0.8 % as total strain. The uniaxial results presented in Fig. 6a) and 6b) indicate that the Jiang's model continues to estimate a lower stress at maximum total strain in the compression region, but in tension the inherent stress is similar to the numerical model estimations. Fig. 6 shows the very first hysteresis loop presented with a dashed line. For the pure axial loading case, the compressive plastic strain and back-stresses are quite similar in both models; however the plastic strains in the tension branch are very different. Jiang's model gives values higher than the experimental results, please see Fig. 6a) and 6d). In the pure shear loading case, the Jiang's model has a hysteresis loop tighter than the experimental results presented here by the numerical simulation for this case. In these cases, the stresses inherent to the shear total strains in compression and tension obtained with the Jiang's model are very similar to the numeric model estimations; moreover the pure axial hysteresis loop is estimated as symmetric by the Jiang model. For the PP loading case, please see Fig. 6c) the Jiang model also gives a symmetrical hysteresis loop. The numerical model displays asymmetrical hysteresis loop for the axial loading. The out-of-phase loading case, Fig. 6d), shows a distorted circle for both numerical analyses; however, the distortion pattern has different directions.

Fig. 7 shows the numerical result for 1.2% of total strain. Due to the high values of the plastic strains involved in this simulation (total strain equal to 1.2%) can be seen that the first hysteresis loop is quite different from the other ones in the

developed numerical model, this indicates the adjustment of the material to the total strain level. The Jiang model continues to estimate the hysteresis loops as symmetric in all loading cases considered here, although the biaxial loading experiments have not yet been made it is expected that the experimental biaxial hysteresis loops be asymmetric and not symmetric as reported by the Jiang's model, once the uniaxial axial hysteresis loops are always asymmetrical. With the increase of the total strain, the inherent stresses estimated by the Jiang's model also increases relatively to the experimental data. This indicates that the Jiang's model does not capture well the total strain level effect on the hysteresis loops shapes. In this case of total strain, 1.2%, the two numerical estimations on the pure shear loading case are very similar having plastic strains and back stress values much alike. Observing the numeric results for the loading cases PP and OP, Fig. 7c) and 7d) can be concluded that, for the first loading cycle, the numerical model and the Jiang's model have a similar behaviour, diverging the results of both models in the subsequent loading cycles.

Fig. 8 presents the numeric results for the 1.4% of total strain, this is a very high strain level leading to the specimen test collapse in a few loading cycles.

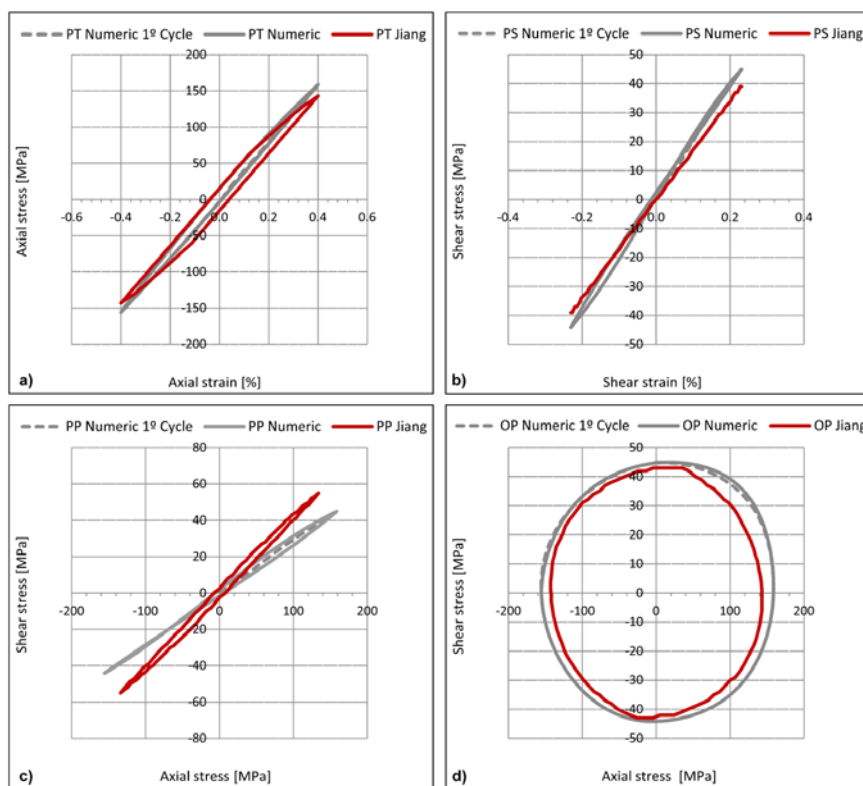For all loading cases it can be seen that the Jiang's hysteresis loops remain symmetric.

Figure 5: Numeric cyclic behaviour comparison between the numeric model developed and the Jiang &Sehitoglu plasticity model for 0.4% as axial strain reference a) PT, b) PS, c) PP and d) OP.

Under an extreme cyclic total strain the Jiang's model presents same plastic strain and back stress values at tension and compression. Which is far from the experimental data, where at the axial loading path the compression load induces high plastic strain and back stresses, moreover the plastic strain in tension is very small comparatively with the one found in compression. For the pure shear loading path, please see Fig. 8d), the experimental hysteresis loop indicates different values for back stresses and plastic strains, which was not seen in lower total shear strains.

From the axial loading case shown in Fig. 8a), it can be seen that the yield stress in compression is much greater than the tension one for the same total strain in tension and compression, which confirms a softening behaviour in tension and a little hardening in compression. Also can be concluded that the Jiang's model is able to estimate well the hardening of the material but unable to deal with its softening. From here can be reinforced the idea which suggests that an experimental and numerical model is needed to establish the different physical phenomena encountered in materials with an hexagonal close packed microstructure (HCP), such as the magnesium alloys.
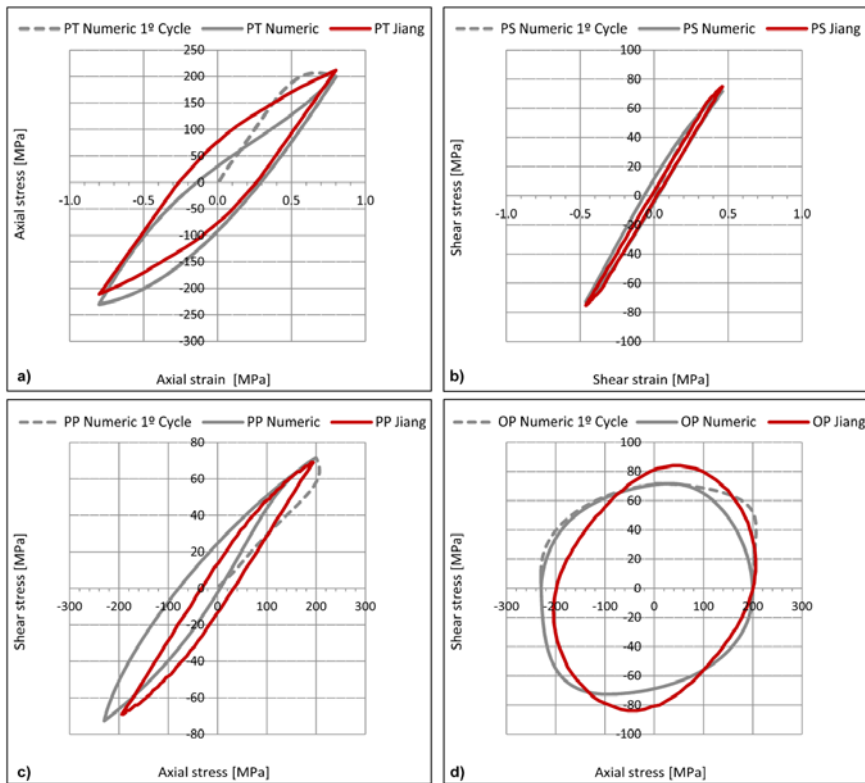
Figure 6: Numeric cyclic behavior comparison between the numeric model developed and the Jiang &Sehitoglu plasticity model model for 0.8% as axial strain reference a) PT, b) PS, c) PP and d) OP.
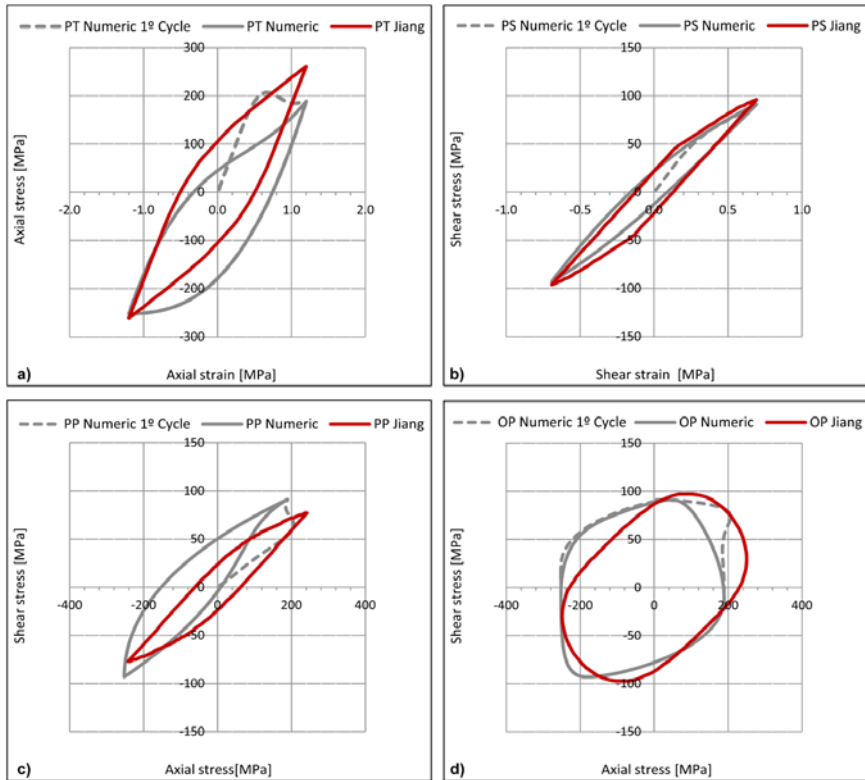

Figure 7: Numeric cyclic behavior comparison between the numeric model developed and the Jiang & Sehitoglu plasticity model for 1.2% as axial strain reference a) PT, b) PS, c) PP and d) OP.
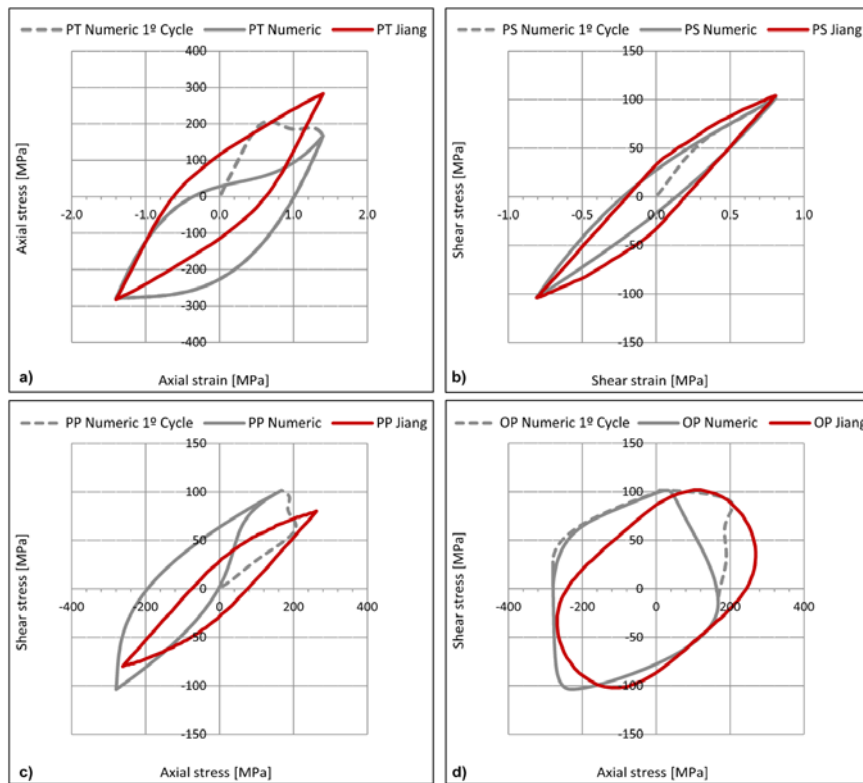
Figure 8: Numeric cyclic behavior comparison between the numeric model developed and the Jiang & Sehitoglu plasticity model for 1.4% as axial strain reference a) PT, b) PS, c) PP and d) OP.

CONCLUSIONS

In this paper was studied the elastic-plastic mechanical behaviour of a magnesium alloy (AZ31B-F) through experimental tests under uniaxial loading conditions. The particular mechanical behaviour inherent to these kinds of materials, hexagonal closed pack microstructures, leads to conclude that it is necessary to have a numeric elastic-plastic model implemented through experimental data. In this context is presented here a first iteration for a numerical model, which modulates the several physical mechanisms inherent to the magnesium elastic-plastic behaviour in uniaxial loading conditions. In order to validate the work already done, numeric estimations were compared with the uniaxial data and with the Jiang & Sehitoglu plasticity model. The numeric results from the implemented model were acceptable; however the Jiang & Sehitoglu model shows some shortcomings on the magnesium hysteresis loop estimations.

ACKNOWLEDGEMENTS

REFERENCES

[1] Sonsino, C.M., Dieterich, K., Fatigue design with cast magnesium alloys under constant and variable amplitude loading, International journal of fatigue, 28 (2006) 183–193.
[2] Anes, V., Reis, L., Li, B., Fonte, M., de Freitas, M., New approach for analysis of complex multiaxial loading paths, International Journal of Fatigue, 62 (2013) 21-33.

[3] Reis, L., Anes, V., de Freitas, M., AZ31 magnesium alloy multiaxial LCF behavior: theory, simulation and experiments, Advanced Materials Research, 891 (2014) 1366-1371.

[4] Anes, V., L. Reis, B. Li, and M. Freitas. "Crack path evaluation on HC and BCC microstructures under multiaxial cyclic loading." International Journal of Fatigue 58 (2014): 102-113.

[5] Anes, V., Reis, L., Li, B., Freitas, M., New approach to evaluate non-proportionality in multiaxial loading conditions, Fatigue & Fracture of Engineering Materials & Structures, (2014). doi: 10.1111/ffe.12192

[6] Armstrong, P.J., Frederick, C.O., A mathematical representation of the multiaxial Bauschinger effect, G. E. G. B., Report RD/B/N, 731, (1966).

[7] Dafalias, Y.F., Popov, E.P., Plastic internal variables formalism of cyclic plasticity, Journal of applied mechanics, 43 (1976) 645–651.

[8] Kurtyka, T., Parameter identification of a distortional model of subsequent yield surfaces, Archives of Mechanics, 40 (1988) 433–454.

[9] Valanis, K.C., A theory of viscoplasticity without a yield surface. II- Application to mechanical behavior of metals(Mechanical response of Al and Cu under complex strain histories conditions, using endochronic theory of viscoplasticity without yield surface), Archiwum Mechaniki Stosowanej, 23 (1971) 535–551.

[10] Lee, M.G., Kim, J.H., Chung, K., Kim, S.J., Wagoner, R.H., Kim, H.Y., Analytical springback model for lightweight hexagonal close-packed sheet metal, International Journal of Plasticity, 25 (2009) 399–419.

[11] Carpinteri, A., Ronchei, C., Spagnoli, A., Vantadori, S., Lifetime Estimation in the Low/Medium-Cycle Regime Using the Carpinteri-Spagnoli Multiaxial Fatigue Criterion, Theoretical and Applied Fracture Mechanics, (2014).

[12] Carpinteri, A., Spagnoli, A., Vantadori, S., Multiaxial fatigue assessment using a simplified critical plane-based criterion, International Journal of Fatigue, 33 (2011) 969–976.

[13] Carpinteri, A., Spagnoli, A., Vantadori, S., Bagni, C., Structural integrity assessment of metallic components under multiaxial fatigue: the C–S criterion and its evolution, Fatigue & Fracture of Engineering Materials & Structures, 36 (2013) 870–883.